Multiple Model Predictive Control for nonlinear systems based on Self-balanced Multi-model Decomposition

Jingjing Du[a,*] , Junfeng Chen[a], Jian Li[a] , Tor Arne Johansen [b]

[a]College of Internet of Things Engineering, Hohai University, Changzhou 213022, China

[b] Department of Engineering Cybernetics, Norwegian University of Science and Technology, NO 7491 Trondheim, Norway

Abstract: A Gap-based Measurement of Nonlinearity (GMoN) is proposed to set up a criterion for multi-model decomposition (MMD) of nonlinear systems. Then a self-balanced multi-model decomposition (SBMMD) approach based on GMoN is put forward for both SISO and MIMO nonlinear systems. Provided an initial value of the threshold and a step-length, a nonlinear system can be automatically partitioned into balanced subsystems: All the subregions have similar GMoNs that are approximated to the final threshold value. Based on the balanced model bank, a balanced multi-model model predictive control (BMMPC) is designed. SISO and MIMO nonlinear systems have been analyzed and synthesized by the proposed SBMMD and BMMPC. It is confirmed that the SBMMD results in a more balanced model bank than other methods. Closed-loop simulations illustrate that the BMMPC has improved closed-loop performance compared to multi-model model predictive controllers (MMPCs) based on less unbalanced model banks. The balanced decomposition helps the BMMPC to achieve consistently good performance in the whole wide operating space.

Keywords: gap metric; GMoN; multi-model decomposition; SBMMD; BMMPC; MIMO nonlinear systems

1 Introduction

Model predictive control (MPC) has been the most successful advanced control technology and has been widely applied in process control because it has superior performance to traditional control methods. Besides, MPC provides a convenient architecture for dealing with multivariable control. However, for a nonlinear chemical system with a wide operating range that exhibits strong nonlinearity, the control performance of a linear MPC controller may degrade. Although nonlinear MPC has been developed for years, it usually includes a nonlinear optimization problem which involves complex and heavy computation [1]. Moreover, it is difficult for control operators to implement a nonlinear MPC. In recent years, the multi-model predictive control method (MMPC), which integrates the merits of the multi-model control approach (MMCA) and MPC, has attracted much attention in controlling nonlinear chemical processes [1-9]. On one hand, the MMPC transforms a complex nonlinear control task into several classical linear ones; while on the other hand, both hard and soft constraints can be directly integrated into the goal function [9].

As well as the MMCA, the MMPC also includes multi-model decomposition (MMD), local controller design (LCD), and combination. MMD is the first and most important [10, 11]. Traditionally, there are mainly three kinds of multi-model decomposition methods [10]: 1) decomposition according to the physical elements, 2) decomposition according to the physical and chemical phenomena, and 3) decomposition according to the operating levels. However, these traditional methods have a common disadvantage: they are reliant on experience or previous

* hzdujing@163.com (Jingjing Du)

knowledge too much [12], making the MMD of a nonlinear system complicated and unsystematic, as the acquisition of experience and previous knowledge may be complicated.

In the past ten years, some systematic decomposition methods have been put forward to enhance efficiency [1, 11-18]. Especially the gap metric, which was used to quantify the distance of two linear systems [19, 20], has been employed to decompose a nonlinear system into subsystems. For example, Galan et al. [11] made use of the gap metric to get a simplified model set for approximating a nonlinear system. Tan et al. [13] made an extension to Galan's method and proposed a decomposition method which connected the selection of sub-models to the H_∞ loop shaping local controller design. Hosseini et al. [14] developed a multiple-model-set identification method based on the H-gap metric. Du et al. [15] proposed a method to determine the minimal number of linear sub-models for approximating a nonlinear system based on the gap metric. Later in 2013, Du et al.[12] extended their method to MIMO nonlinear systems and developed an MMD method based on gap metric. In 2014, the gap metric and the stability margin were employed to perform the MMD and LCD simultaneously, and later the idea was extended to MMPC of MIMO nonlinear systems [1]. In 2017, the gap metric was used to formulate a control-relevant nonlinearity measure (CRNM) method, and an integrated MMCA based on CRNM was proposed, in which local controllers were designed during the division of the nonlinear systems [17]. In [18], a state-space partition method integrated with an optimal control method proposed for hybrid nonlinear systems. And some researchers have introduced the network theory into control field and proposed some systematical decomposition methods for large-scale complex processes. For example, in [19], Daoutidis et al. proposed a systematical decomposition method based on community detection. They analyzed the interaction among variables (inputs, states, and outputs) and constraints, partitioned the variables and constraints into groups, and decompose the processes into subsystems. And then distributed MPC is designed based on the subsystems for the large-scale systems. A distributed MPC based on community detection decomposition reduces the computational time and has fewer communication requirements, and good resilience to faults [20]. Later in [21], they proposed a systematic method to decompose the integrated scheduling and dynamic optimization problem using the community detection. And the resulted optimization can be solved faster than the original monolithic complex problem. In [22], Zavala et al. proposed an overlapping Schwarz decomposition method for network systems or systems that can be modeled by Graph. The method has better convergence performance than alternating direction method of multipliers and Jacobi/Gauss-Seidel for some types of systems [23].

The above methods made improvement on the traditional methods. Dependency on experience and previous knowledge was reduced, and the efficiency of decomposition was raised. Besides, the closed-loop performance was improved because of better local model selection. However, there still exist some drawbacks in the above MMD methods. For example, the community detection decomposition methods and overlapping Schwarz decomposition method are designed for large-scale processes with lots of variables and constraints but a limited operating range. Based on these decompositions, decentralized control is employed. Here in our work, we focus on the nonlinear systems with a wide operating range, for which MMCA is employed to design a controller. For the above gap-metric-based methods, either a definite threshold value is necessary [11-15, 18] or local controller design is involved in the MMD process [16-18]. When local controller design is involved, the decomposition process becomes

complex as tuning of a controller's parameters is not trivial. If the MMD needs a definite threshold value, repetitive trials and tests are needed before a proper threshold value is obtained, which makes the MMD complicated and less efficient. Besides, there is no criterion to test whether the decomposition result is good or bad before an open-loop model validation (OLMV) [12, 14, 15] or a closed-loop control simulation (CLCS) [11, 13, 16-18] is made. However, neither the OLMV nor the CLCS is trivial. What's more, these tests are done afterward. If the decomposition is not satisfactory, the decomposition process has to be done at least once again, which makes the division process rather complex. In addition to these drawbacks, there is one more disadvantage in the existent MMD methods. It is that the division is unbalanced： some subregions are too narrow and others are too wide. In other words, the nonlinearity of the considered system in some subregions is much bigger than in others. These shortcomings may have a bad influence on the subsequent local and global controller design. Since the nonlinear system in different subregions has different degrees of nonlinearity, the local controllers usually have different performances in dynamics, stability and robustness. After weighted summation, the resulted multi-model controller may have an unbalanced performance in different subregions. That is to say, in some operating levels, the multi-model controller (MMC) performs well, while in other operating levels the MMC performs not well. Therefore, making the nonlinear system in each subregion has similar nonlinearity (defined according to a certain criterion) is important for improving the closed-loop control performance of a multi-model controller.

To overcome the above mentioned drawbacks, the following goals are taken into consideration when performing the MMD of a nonlinear system for the first time in this work: (1) To set up a criterion, *i.e.* the GMoN, for MMD using the gap metric. (2) To further simplify the MMD process and make the MMD process as automatic as possible. (3) To make the decomposition as balanced as possible in terms of the criterion. Therefore, a self-balanced multi-model decomposition (SBMMD) method is put forward in this work. Different from the existent MMD methods, in the proposed SBMMD method, a proper threshold value can be found via iteration and the multi-model partition of a nonlinear system can be done almost automatically. Especially, a criterion based on the GMoN for decomposition is set up, so that local models are obtained according to the same criterion, and a balanced decomposition can be obtained automatically. Thus a balanced linear model bank is acquired and local MPCs are designed on basis of them. The balanced model bank will help to improve the closed-loop performance of the global multi-model controller. Because the balanced model bank helps to make the local controllers perform similarly, thus their combination can have consistent closed-loop performance in the whole operating space. Several nonlinear systems are analyzed and synthesized to demonstrate that the proposed methods are effective and helpful.

This paper is organized as follows. Section 2 introduces a measurement of nonlinearity based on gap metric, i.e., GMoN (gap-based measurement of nonlinearity) for short. In Section 3, an SBMMD method is proposed via two algorithms for SISO and MIMO nonlinear systems, respectively. Several nonlinear systems are investigated to illustrate the SBMMD method. In Section 4, a BMMPC method is developed based on the proposed balanced decomposition in Section 3. In Section 5, closed-loop simulations are present to demonstrate the usefulness and effectiveness of the SBMMD and BMMPC, and in Section 6 conclusions are made.

2 Gap metric and GMoN

In this section, the gap metric theory is briefly reviewed and a measurement of nonlinearity based on it is proposed in order to set up a criterion for MMD.

2.1 Gap metric

The gap metric between two linear systems P_1 and P_2 with their normalized right coprime factorizations: $P_1 = N_1 M_1^{-1}$ and $P_2 = N_2 M_2^{-1}$ is defined by (1). Details can be found in [24, 25].

$$\delta(\mathrm{P}_1,\mathrm{P}_2) = \max\left\{\vec{\delta}(\mathrm{P}_1,\mathrm{P}_2)\vec{\delta}(\mathrm{P}_2,\mathrm{P}_1)\right\} \tag{1}$$

where $\vec{\delta}(\mathrm{P}_1,\mathrm{P}_2) = \inf_{\mathrm{Q}\in \mathrm{H}_\infty}\left\|\begin{bmatrix}\mathrm{M}_1\\ \mathrm{N}_1\end{bmatrix} - \begin{bmatrix}\mathrm{M}_2\\ \mathrm{N}_2\end{bmatrix}\mathrm{Q}\right\|_\infty$ and $\vec{\delta}(\mathrm{P}_2,\mathrm{P}_1) = \inf_{\mathrm{Q}\in \mathrm{H}_\infty}\left\|\begin{bmatrix}\mathrm{M}_2\\ \mathrm{N}_2\end{bmatrix} - \begin{bmatrix}\mathrm{M}_1\\ \mathrm{N}_1\end{bmatrix}\mathrm{Q}\right\|_\infty$ are two directed gaps, and they can be computed by solving two H_∞ optimization problems [25].

The gap metric has a list of merits [11, 13]. First of all, the value of the gap metric is within [0, 1], making it more intuitive and suitable than a norm-based metric [25]. Secondly, the gap metric is helpful for system analysis and synthesis. When the gap metric between two systems is near one, it is difficult to design a linear controller to stabilize them both. Otherwise, when the gap is near zero, the two systems have similar dynamics and a linear controller can be found for them both. As a result of these properties, the gap metric is employed to define a criterion for MMD in the following.

2.2 Gap-Metric-based Measurement of Nonlinearity (GMoN)

Measurement of nonlinearity, i.e., to measure the nonlinearity degree of a nonlinear system, also called nonlinearity measure, is an important concept in nonlinear control systems [26-39]. In this work, a GMoN method based on the merits of the gap metric is proposed to set up a criterion for MMD for nonlinear systems. For interpreting the concept clearly, the GMoN is defined for SISO and MIMO systems separately.

2.2.1 GMoN for SISO nonlinear systems

Consider the nonlinear system represented in (2):

$$\begin{cases}\dot{x} = f(x,u,\theta)\\ y = g(x,u,\theta)\end{cases} \tag{2}$$

where x, u, y are the state, control input, and the output variables, respectively. θ is the scheduling variable(s), and $f(\cdot)$, $g(\cdot)$ are nonlinear functions that are differentiable.

Suppose (2) is a **SISO nonlinear system** in this subsection. Its scheduling variable θ is chosen according to the principles in [40]. Then the system is gridded by the gap-metric-based dichotomy algorithm [12]. Assume n gridding points (GPs) $\theta = [\theta_1, \theta_2, \theta_i \ldots, \theta_n]$ are obtained. Then each GP is a steady-state point (SSP) of the system (2). The SSP for θ_i is $(x_0(\theta_i)\ u_0(\theta_i)\ y_0(\theta_i)) := (x_{0i}, u_{0i}, y_{0i})$. Then system (2) is linearized and discretized around (x_{0i}, u_{0i}, y_{0i}) with sampling interval T_s. The linearized and discretized model G_i is described by:

$$\begin{cases}x_i'(k+1) = A_i x_i'(k) + B_i u_i'(k)\\ y_i'(k) = C_i x_i'(k) + D_i u_i'(k)\end{cases} \qquad i = 1, \ldots, n \tag{3}$$

where $x_i'(k)$ denotes the state variable; $x_i'(k) = x(k) - x_{0i}$, $u_i'(k) = u(k) - u_{0i}$, $y_i'(k) = y(k) - y_{0i}$; A_i, B_i, C_i, and D_i are the linearized and discretized matrix of G_i around (x_{0i}, u_{0i}, y_{0i}) of nonlinear system (2) .

Compute the gap metric between every pair of the n linearized models, such that a matrix $\Delta = [\delta_{ij}]_{n\times n}$ is acquired. Then the best local linear model (BLLM) G^* among the n linearized models G_i (i = 1, 2, 3, …, n) is selected according to the mix-max principle [17] in (4):

$$G^* = \{G_j : min_{1 \le j \le n}(max_{1 \le i \le n}\delta(G_j, G_i))\} \quad (4)$$

The maximal one of the n gap metrics between G^* and the n models is defined as the gap-based measurement of nonlinearity (GMoN) in the region:

$$\text{GMoN} := \delta_{max}(G^*) = max_{1 \le i \le n}\delta(G^*, G_i) \quad (5)$$

The above is the definition of the GMoN for SISO nonlinear systems. In the subsequent, the GMoN for MIMO systems will be defined.

2.2.2 GMoN for MIMO nonlinear systems

Computation of the GMoN of a MIMO nonlinear system that has multiple scheduling variables is much more complicated than a SISO nonlinear system with a single scheduling variable. In this subsection, MIMO nonlinear systems with two scheduling variables are investigated to illustrate the definition and computation of the GMoN of MIMO systems. Systems with more scheduling variables are under research.

In this section, suppose (2) is a MIMO nonlinear system with two scheduling variables α and β. Let the gridding result be $\alpha = [\alpha_1, \alpha_2, \ldots, \alpha_m]$, $\beta = [\beta_1, \beta_2, \ldots, \beta_n]$ after gridding using the method from [12]. As illustrated in Figure 1, each combination (α_i, β_j) relates to only one SSP in the operating range. Define a subsystem $G(\alpha_i, \beta_j)$ around (α_i, β_j) by linearizing the nonlinear system (2), where $G(\alpha_i, \beta_j)$ is shorted as $G(i, j)$ for simplicity of notation, i=1,2,…,m, j=1,2,…,n. Hence, there are a total of $n \times m$ linearized models. Then calculate the gap metric of every pair of models and a four-dimensional gap metric matrix $\Delta = [\delta_{ijtl}]_{n \times m \times n \times m}$ is obtained.

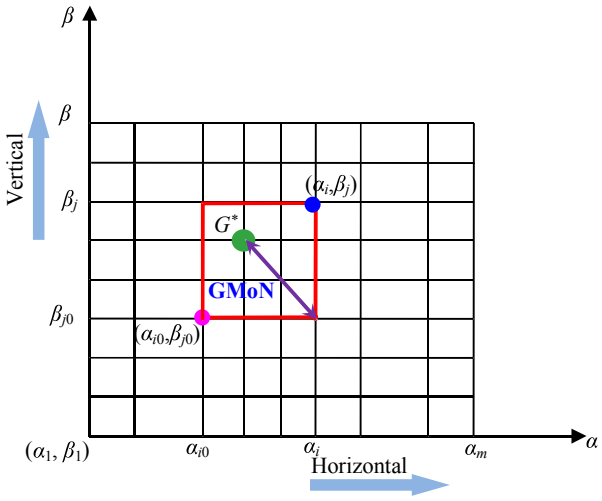

Figure 1. The definition and computation of GMoN for MIMO systems

As illustrated in Figure 1, suppose the area in the red rectangle is the considered operating region. The initial point is $(\alpha_{i0}, \beta_{j0})$ and the final point is (α_i, β_j). Every combination of α_{i0} , $\alpha_{i0+1}, \ldots, \alpha_i$ and $\beta_{j0}, \beta_{j0+1}, \ldots, \beta_j$ corresponds to a linearized model. Thus there are a total of $(i\text{-}i_0+1) \times (j\text{-}j_0+1)$ linearized models in this operating region. Find out the maximal gap related to every linearized model in the matrix Δ. For instance, as to the model $G(z, l)$ $(i_0 \le z \le i,\ j_0 \le l \le j)$, define the maximal gap corresponding to $G(z, l)$ as follows:

$$\Delta_{zl} := \max_{\substack{i_0 \le s \le i \\ j_0 \le t \le j}} \delta(G(z,l), G(s,t)) \quad (6)$$

Thus Δ_{zl} is the maximal gap related to model $G(z, l)$. Then for the $(i\text{-}i_0+1)\times(j\text{-}j_0+1)$ linearized models, a **max-gap-matrix**, $\Lambda\coloneqq[\Delta_{zl}]_{(i-i_0+1)\times(j-j_0+1)}$ is obtained, and the best local linear model (BLLM) G^* of this region (i.e., the area in the red rectangle) is selected in the following sense:

$$G^* = \{G(v,h):\Delta_{vh} = \min(\min(\Lambda))\} \tag{7}$$

Then the GMoN of the nonlinear system in this operating region is:

$$\mathrm{GMoN}\coloneqq\min(\min(\Lambda)) \tag{8}$$

Eqs. (7) and (8) are the definition and computation of the GMoN for a MIMO nonlinear system that has two scheduling variables.

It is noted that the definition and computation of the GMoN is directly related to the operating region of the considered nonlinear system. Therefore, once the GMoN of a nonlinear system is to be calculated, the operating space should be defined. So it can be called the GMoN of the region. As the GMoN is computed based on the BLLM, we also call "the GMoN of the BLLM" for simplicity of statement in the following sections. The nonlinearity degree of nonlinear systems with more scheduling variables can be measured in the same way with more computational effort. According to the implication of the gap metric, if the GMoN of a nonlinear system is bigger than 0.6, it usually means the system exhibits strong nonlinearity and a linear controller is insufficient for it [12].

With the definition and computation of the GMoN, a self-balanced MMD method will be put forward for both SISO and MIMO nonlinear systems in Section 3.

3 Self-balanced multi-model decomposition

In this work, a self-balanced decomposition method is proposed using the GMoN as a measuring tool to avoid the drawbacks involved in the current gap-based multi-model decomposition reviewed in Section 1. The detailed method is summarized into two algorithms for SISO and MIMO nonlinear systems, respectively.

3.1 SBMMD Algorithm for SISO nonlinear systems

For a SISO nonlinear system, n linearized models G_i (i = 1, 2,…, n) are set up as in (3) after gridding, linearization, and discretization before a gap-matrix $[\delta_{ij}]_{n\times n}$ is computed. Then the self-balanced decomposition algorithm for SISO systems is summarized in Algorithm1.

Algorithm 1: SBMMD for SISO nonlinear systems

S1. Choose an initial value ξ_0 and a step-length ζ.

S2.Set $\xi = \xi_0$ and $\eta = 1$.

S3. Set $i = 1$ and $m_\eta = 0$.

S4. If $i \le n$, let $j = i$ and $m_\eta = m_\eta + 1$, and go to S5. Otherwise jump to S12.

S5. Choose the BLLM G^* in accordance with (9).

$$G^*\coloneqq\{G_z:\min_{i\le z\le j}(\max_{i\le l\le j}(\delta(G_z,G_l)))\} \tag{9}$$

S6. Compute the GMoN of the BLLM according to (10).

$$\mathrm{GMoN}\coloneqq\max_{i\le z\le j}\left(\delta\left(G^*,G_z\right)\right) \tag{10}$$

S7. If $\mathrm{GMoN}\le\xi$, set $j = j + 1$ and return to S5.

S8. Otherwise if $\mathrm{GMoN} > \xi$, Set $j = j - 1$.

S9. Update the BLLM using (9).

S10. The BLLM G^* is noted as $P_{m\eta}$, and its grid point is noted as $OP_{m\eta}$. Put $P_{m\eta}$ into Queue pQ_η, and $OP_{m\eta}$ into Queue opQ_η

S11. Let $i = j + 1$, and return to S4.

S12. If $\eta > 1$ and $m_\eta > m_{\eta-1}$, go to S14. Otherwise, go to S13.

S13. Let $\xi = \xi - \zeta$ and $\eta = \eta + 1$. And return to S3.

S14. The self-balanced decomposition is completed. The final threshold value is $\xi = \xi + \zeta$. The nonlinear system is partitioned into $m_{\eta-1}$ local models, with the local models $pQ_{\eta-1}$ and operating points $opQ_{\eta-1}$.

Remark 1: ξ is threshold value of decomposition. Its initial value ξ_0 can be chosen around 0.6 according to our experience.

Remark 2: ζ can be chosen between 0.001 and 0.01.

Remark 3: η is the number of iterations and m_η is number of sub-models in the ηth iteration.

Remark 4: From S7-S9 in Algorithm 1, it can be seen that the GMoN is used as the division criterion. Only when the GMoN of the operating area is near to, but smaller than, the threshold value, the operating area is wide enough to be a subregion. Therefore, it is guaranteed that each subregion has a similar GMoN. This is the key to get a balanced decomposition.

Remark 5: In S12-S13, the selection of a proper threshold value is realized through the iterative procedure. Once the number of sub-models increases in comparison with the previous decomposition, it means the newly added local model has a rather smaller GMoN than others. Therefore, it is not balanced, so the algorithm will go back to the previous decomposition. The previous decomposition is then the best and balanced one regarding the GMoN.

Since the decomposition is done by using the GMoN as the partition criterion, the nonlinear system is decomposed while the decomposition result is tested in terms of the GMoN. Therefore, the MMD of a nonlinear system is simplified and improved. When the local models have similar GMoNs, it is expected that the local controllers have similar performance. Furthermore, it helps to make the multi-model controller have consistent (stability and robustness) performance in the whole operating level.

In the next section, the proposed Algorithm 1 will be applied to two SISO nonlinear systems to illustrate its effectiveness.

3.2 SISO Case studies

In this section, two different continuous stirred tank reactor (CSTR) systems are modeled by the self-balanced decomposition method, and comparisons have been made with other decomposition methods.

3.2.1 An exothermic CSTR (eCSTR)

Consider an eCSTR, where an irreversible, first-order reaction takes place [11]. The nonlinear dynamics of the eCSTR process are in (11):

$$\begin{cases} \dot{x}_1 = -x_1 + D_a(1 - x_1)\exp\left(\frac{x_2}{1 + x_2/\gamma}\right) \\ \dot{x}_2 = -x_2 + BD_a(1 - x_1)\exp\left(\frac{x_2}{1 + x_2/\gamma}\right) + \vartheta(u - x_2) \\ y = x_2 \end{cases} \tag{11}$$

where the state x_1 is the dimensionless reagent conversion; the state x_2 is reactor temperature; and the input u is the coolant temperature. All the variables are dimensionless. The values of the parameters in (11) are $D_a = 0.072$, $\gamma = 20$, $B = 8$, and $\vartheta = 0.3$.

As seen in Figure 2, the eCSTR exhibits strong output multiplicity. y is selected as the

scheduling variable as it reflects the system's nonlinearity, where $\{y|y \in [0,6)\}$ is the entire operating range. Applying the gridding algorithm [12] to the eCSTR, 58 GPs are resulted to grid the eCSTR process, as shown in Figure 2.

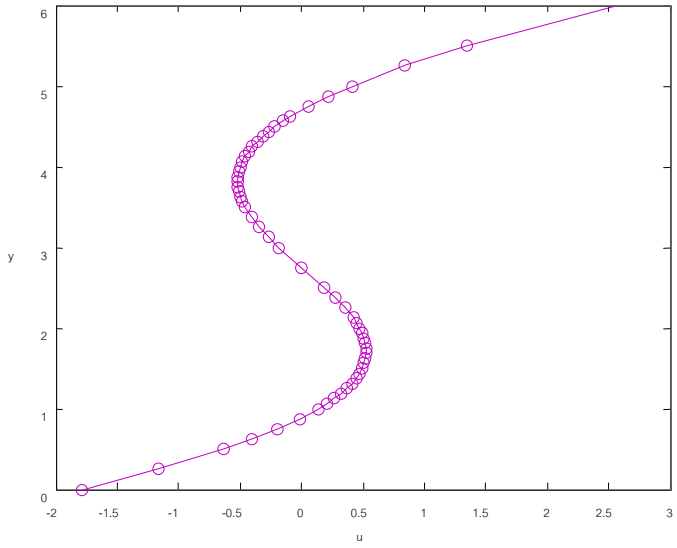

Figure 2. Gridding result of the eCSTR with 58 GPs

For the 58 GPs, 58 linearized models are built and the 58×58 gap-matrix is computed. Then P_{10} is chosen as the BLLM according to (4) and the GMoN according to (5) is:

$$\text{GMoN} := \delta_{max}(P_{10}) = 0.7971$$

Since $0.7971 > 0.5$, the eCSTR is strongly nonlinear, and a linear controller is insufficient in the whole operating space. Applying the proposed balanced multi-model decomposition method, Algorithm 1with ξ_0 =0.6 and $\zeta = 0.01$, to the eCSTR system, the partition result is in Table 1 with the final threshold value as $\xi = 0.52$. The eCSTR system is decomposed into three submodels. Three submodels are the best for multi-model control of the eCSTR system considering both control performance and computational effort [16,17].

Table 1 Self-balanced multi-model decomposition of the eCSTR

Subregion	1st	2nd	3rd
Linearized models	1→17	18→42	43→58
Operating point of BLLM ($[x_1, x_2]'$, u)	11st ([0.1809,1.1875]', 0.3214)	22nd ([0.6183,3.6875]', -0.509)	50th ([0.755,4.625]', -0.0907)
Subrange	$0 \le y <1.5625$	$1.5625 \le C_A <4.125$	$4.125 \le C_A <6$
GMoN	0.5054	0.5180	0.5112

Table 1 is interpreted as follows: the 1st to 17th grid points are classified into the 1st subregion; the operating point (OP) for the 1st subregion is the 11th GP: ($[x_1, x_2]'$, u) = ([0.1809, 1.1875]', 0.3214); and the operating space of the 1st subregion is $\{y|0 \le y < 1.5625\}$. The GMoN of the 1st subregion is $\text{GMoN}_1 = 0.5054$. The 18th to 42nd grid points belong to the 2nd subregion with the 22nd grid point ($[x_1, x_2]'$, u) = ([0.6183, 3.6875]', -0.509) as its OP, the subrange is $\{y \,|1.5625 \le y < 4.125\}$, and $\text{GMoN}_2 = 0.5180$. The 3rd subregion includes the linearized models 43-58; and the

OP is ([x_1, x_2]', u) = ([0.755, 4.625]', -0.0907); and it covers the space $\{y \mid 4.125 \le y < 6\}$, and $GMoN_3$ = 0.5112. We note that the three subregions have similar values of the GMoN, and the decomposition is balanced in terms of the GMoN.

The matrices for the BLLMs are listed as follows:

$$A_1 = \begin{bmatrix} -1.2209 & 0.1612 \\ -1.7670 & -0.0104 \end{bmatrix},\ B_1 = \begin{bmatrix} 0 \\ 0.3 \end{bmatrix},\ C_1 = [1\ 0],\ D_1 = [0],$$

$$A_2 = \begin{bmatrix} -2.6199 & 0.4408 \\ -12.9592 & 2.2263 \end{bmatrix},\ B_2 = \begin{bmatrix} 0 \\ 0.3 \end{bmatrix},\ C_2 = [1\ 0],\ D_2 = [0],$$

$$A_3 = \begin{bmatrix} -4.0810 & 0.4980 \\ -24.6480 & 2.6840 \end{bmatrix},\ B_3 = \begin{bmatrix} 0 \\ 0.3 \end{bmatrix},\ C_3 = [1\ 0],\ D_3 = [0].$$

In subsequent sections, local MPCs are designed using these parameters.

For comparison, the GMoNs of the local regions of the same eCSTR process in [15] are computed: $GMoN_1$ = 0.5610; $GMoN_2$ = 0.5922; $GMoN_3$ = 0.3610.

The GMoNs of the subregions of eCSTR process in [17] can be found in Table 13 in [17]. They are: $GMoN_1$=0.6780; $GMoN_2$=0.4332; $GMoN_3$=0.5249.

It is clearly seen that the decomposition in Table 1 is the most balanced for the eCSTR process in terms of the GMoN. All of the 3 subregions have similar GMoNs approximating the final threshold of 0.52. However, $GMoN_3$ of the 3rd subregion in [15] is much smaller than the other two, and also smaller than the threshold value of 0.6. In [17], the eCSTR is partitioned using an integrated MMD algorithm. The GMoNs are less balanced, too.

3.2.2 An isothermal CSTR (iCSTR)

Consider an iCSTR, where a first-order irreversible reaction takes place [13]. The system is described by (12).

$$\frac{dC_A}{dt} = -k_r C_A + (C_{Ai} - C_A)u \tag{12}$$

where C_A, u are the state and input, respectively, and the constants are C_{Ai} = 1.0 and k_r = 0.028 min^{-1}.

It has been pointed out that the iCSTR is strongly nonlinear [17] as seen from the static equilibrium curve which has an almost 90-degree change in the output direction. Here the GMoN is applied to the iCSTR to measure its nonlinearity.

First of all, the iCSTR process is gridded via the dichotomy method [12] and 19 GPs is obtained as shown in Figure 3. Then the iCSTR system is linearized and discretized around the 19 gridding points and 19 linearized models are acquired. Calculating the gap-matrix and getting the BLLM model, the GMoN is obtained as follows.

$$\text{GMoN} := \delta_{max}(P_{10}) = 0.7551$$

Since $0.7551 > 0.5$, a linear control is unable to control the iCSTR in the entire operating region. Applying Algorithm 1 to the iCSTR with ξ_0 = 0.6 and ζ = 0.01, the decomposition result is in Table 2 with $\xi = 0.46$. If ξ_0 = 0.5 is used instead of 0.6, the decomposition result is the same as in Table 2. Therefore, the SBMMD algorithm is not sensitive to the initial value of the threshold.

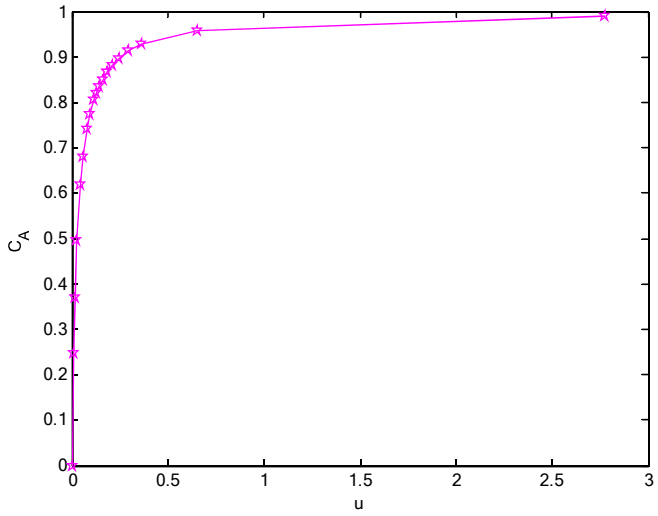

Figure 3. Gridding of iCSTR with 19 GPs

Table 2 Self-balanced multi-model decomposition of the iCSTR

Subregion	1st	2nd
Linearized models	1→9	10→19
Operating point of BLLM (C_A, u)	5th (0.6187, 0.0454)	14th (0.8817, 0.2087)
Subrange	$0 \le C_A < 0.804$	$0.804 \le C_A < 1$
GMoN	0.4536	0.4439

As is shown in Table 2, the iCSTR system is decomposed into two submodels. Two submodels are the best for multi-model control of the iCSTR system considering both control performance and computational effort [16,17].

The decomposition in Table 2 is balanced as the two local models have similar GMoNs that are close to the final threshold of 0.46. The state-space model matrices for the BLLMs are listed as follows:

$$A_1 = -0.0734,\ B_1 = 0.3813,\ C_1 = 1, D_1 = 0,$$

$$A_2 = -0.2367,\ B_2 = 0.1183,\ C_2 = 1, D_2 = 0.$$

For comparison, the GMoNs of the local regions in [15] are shown here.

$$GMoN_1 = 0.5902; \quad GMoN_2 = 0.2985;$$

And in [17], the GMoNs of the two local regions are:

$$GMoN_1 = 0.6527; \quad GMoN_2 = 0.1785;$$

Therefore, the decomposition in Table 2 is the most balanced of the three. Besides, the proposed decomposition is carried out almost automatically while the other methods may need repetitive tuning of parameters or re-decomposition several times before a satisfactory result is obtained. Moreover no OLMV/CLCS tests are needed afterward since the proposed self-balanced decomposition using the GMoN as a criterion during the decomposition process.

Simulations in section 5 will demonstrate that the balanced decomposition helps to improve the closed-loop performance and make our BMMPC has consistent performance in the whole operating space.

3.3 Algorithm for MIMO nonlinear systems with two scheduling variables

A total of $n \times m$ linearized models are built after gridding, linearization, and discretization for a MIMO system with two scheduling variables α and β, where a **four-dimensional** matrix $[\delta_{ijtl}]_{n \times m \times n \times m}$ is computed. Then the SBMMD for MIMO systems is summarized in Algorithm 2.

Algorithm 2: SBMMD for MIMO nonlinear systems

Sm1. Select an initial distance level ξ_0 and a step-length ζ.

Sm2. Let $\xi = \xi_0$ and $\eta = 1$.

Sm3. Let $i_0 = 1, j_0 = 1, m_\eta = 0$, $flag_h = 0$, and $flag_v = 0$.

Sm4. Set $i = i_0, j = j_0$, $G_0 = G(i_0, j_0)$,

Sm5. For $i \le m$ *and* $j \le n$, set $m_\eta = m_\eta + 1$, and go to Sm6. Otherwise jump to Sm12.

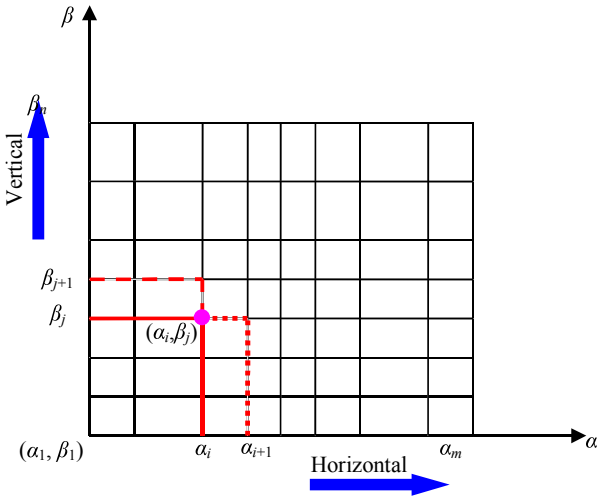

Figure 4. SBMMD for MIMO nonlinear systems

Sm6. Horizontal direction: Let $i = i + 1$, and the crossover GPs in the dotted line in Figure 4 is added into the current subregion. Then there are a total of $(i\text{-}i_0+1)\times(j\text{-}j_0+1)$ GPs for all of the combination of α_{i0} , α_{i0+1}, …, α_i, and $\beta_{j0}, \beta_{j0+1}, \ldots, \beta_j$. Choose the BLLM G^* according to (7) and compute the GMoN according to (8).

If $GMoN > \xi$, let $i = i - 1$.

If $GMoN > \xi$, or $i > m$, let $flag_h = 1$.

Sm7. (1) If $flag_h = 0$ and $flag_v = 0$, jump to Sm8.

(2) If $flag_h = 0$ and $flag_v = 1$, jump to Sm6.

(3) If $flag_h = 1$ and $flag_v = 0$, jump to Sm8.

(4) If $flag_h = 1$ and $flag_v = 1$, jump to Sm10.

Sm8. Vertical direction: Let $j = j + 1$, and the $(i\text{-}i_0+1) \times (j\text{-}j_0+1)$ crossover GPs in the dashed line in Figure 4 are moved into the current subregion. Choose the BLLM G^* according to (7) and compute the GMoN according to (8).

If $GMoN > \xi$, let $\mathrm{j} = \mathrm{j} - 1$.

If $GMoN > \xi$ or $\mathrm{j} > n$, let $flag_v = 1$.

Sm9. (1) *If* $flag_h = 0$ *and* $flag_v = 0$, jump to Sm6.

(2) *If* $flag_h = 0$ *and* $flag_v = 1$, jump to Sm6.

(3) *If* $flag_h = 1$ *and* $flag_v = 0$, jump to Sm8.

(4) *If* $flag_h = 1$ *and* $flag_v = 1$, jump to Sm10.

Sm10. The BLLM G^* is denoted as $P_{m\eta}$, and its GP is denoted as $OP_{m\eta}$. Put $P_{m\eta}$ into Queue pQ_η, and $OP_{m\eta}$ into Queue opQ_η

Sm11. Select a new beginning point, a vertex of the previous subregions. Set $flag_h = 0$ and $flag_v = 0$, and go back to Sm4.

Sm12. If $\eta > 1$ and $m_\eta > m_{\eta-1}$, go to Sm14. Otherwise, go to Sm13.

Sm13. Set $\xi = \xi - \zeta$ and $\eta = \eta + 1$, and return to Sm4.

Sm14. The self-balanced decomposition is completed. Finally $\xi = \xi + \zeta$. The nonlinear system is partion into $m_{\eta-1}$ subsystems. And model bank is $pQ_{\eta-1}$ and operating points are $opQ_{\eta-1}$.

Remark 6: Note that the horizontal division is done first whenever it is possible. Only when the horizontal division is done, the vertical division is started.

Remark 7: Note that in our method, the subregions are rectangles for the simplicity of the MMD algorithm and the regularity of the shapes of the subreigons.

Remark 8: From the above description, it is clear that the main features of the proposed SBMMD lie in two aspects. (1)Use the GMoN as a criterion, and make each local subregion have similar values of the GMoN. Thus a balanced partition is resulting. Therefore, lack of partition criterion, result test after decomposition, and unbalanced decomposition are avoided. (2)Use an iterative procedure to get a proper threshold value for partition, so an initial threshold and a step-length are enough. Repetitive trials and complex parameter tuning are then avoided. In short, the drawbacks of the current decomposition methods are reduced.

3.4 An MIMO CSTR process

Consider a constant volume mCSTR cooled by a single coolant stream, where an irreversible, exothermic reaction, A→B, takes place [1]. Its mathematical model is given in (13).

$$\begin{cases} \dot{C}_A(t) = \frac{q}{V}[C_{A0} - C_A(t)] - k_0 C_A(t) e^{-\frac{E}{RT(t)}} \\ \dot{T}(t) = \frac{q}{V}[T_0 - T(t)] + k_1 C_A(t) e^{-\frac{E}{RT(t)}} + k_2 q_c(t)\left[1 - e^{-\frac{k_3}{q_c(t)}}\right][T_{c0} - T(t)] \end{cases} \tag{13}$$

The input variables of the system are q and q_c, and the output variables are C_A and T. The parameters in (13) are given in [1]. The ranges of the variables are $q \in [95,150]$,$q_c \in [60,110]$, $C_A \in [0.02, 0.15]$, and $T \in [430,490]$.

It is pointed out in [1] that the mCSTR operates in a wide range and a linear controller is insufficient for it in the entire operating range. Therefore, the proposed GMoN will be applied to the mCSTR process to compute its nonlinearity level, and the self-balanced decomposition Algorithm 2 will be employed to partition it into linear local models. Then MMPC is designed based on the models in Section 5.

For the mCSTR system, the pair (q, q_c) captures the system's nonlinearity at equilibrium. Thus q and q_c are chosen as scheduling variables. Using the dichotomy method [12], the gridding results of the mCSTR process are shown in Figure 5 and Figure 6. The GPs in q direction are 33 GPs, and in q_c direction there are 24 GPs.

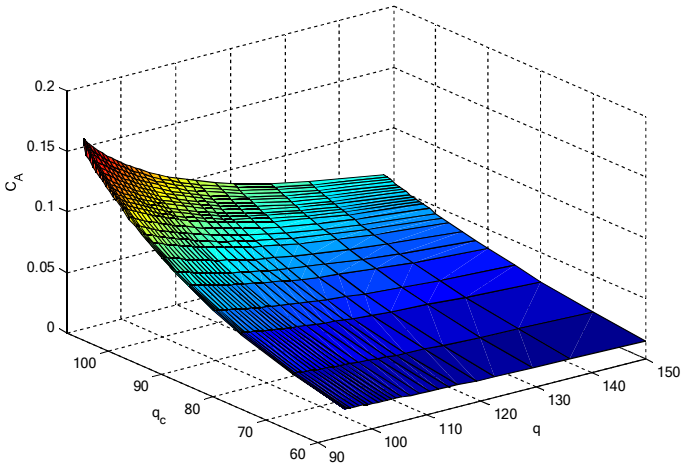

Figure 5. Gridding of mCSTR (C_A)

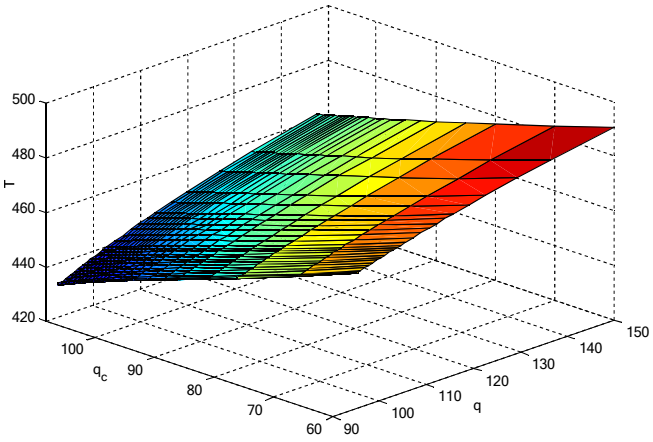

Figure 6. Gridding of mCSTR (T)

Based on the gridding result, the GMoN of the mCSTR system is computed according to (7) and (8).

$$\mathrm{GMoN} = 0.6917$$

Since it is larger than 0.6, this mCSTR process exhibits strong nonlinearity. We apply the proposed Algorithm 2 to this mCSTR with $\xi_0 = 0.6$ and step-length $\zeta = 0.01$. The decomposition is shown in Figure 7. Details of the decomposition are summarized in Table 3. The mCSTR system is decomposed into three submodels. Three submodels are the best for multi-model control of the mCSTR system considering both control performance and computational effort [1, 12].

Table 3 Self-balanced multi-model decomposition of the mCSTR with final threshold $\xi = 0.5$

Subregion	1st	2nd	3rd
Linearized models	H:1→18 V:1→17	H:18→33 V: 1→24	H:1→18 V: 17→24

Operating point of BLLM (C_A, T, q, q_c)	OP_1 (11,10) (0.09658,438.47 95.895,100)	OP_2 (18,12) (0.092869,440.48, 101.88,102.5)	OP_3 (9,18) (0.126,432.67, 95.215,106.25)
Subrange	$\begin{cases}95 \le q < 101.9\\ 60 \le q_c < 105.6\end{cases}$	$\begin{cases}101.9 \le q < 150\\ 60 \le q_c < 105.6\end{cases}$	$\begin{cases}95 \le q < 101.9\\ 105.6 \le q_c < 110\end{cases}$
GMoN	0.4800	0.4985	0.4458[0.4897]

In Table 3, "H: 1→18"means, in the horizontal direction, i.e. the 1st-18th gridding points of q. And "V: 1→17"means, in the vertical direction, i.e. the 1st-17th gridding points of q_c. The other contexts in Table 3 are interpreted similarly as Table 1. The systematic matrixes of three BLLMs are omitted for brevity.

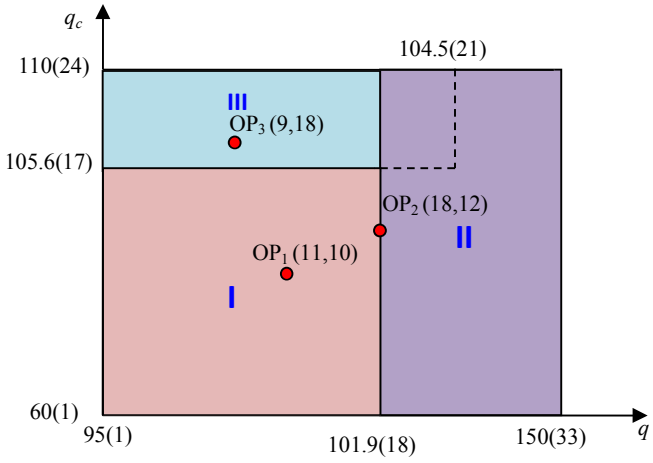

Figure 7. Self-balanced decomposition result of the mCSTR process

In the self-balanced decomposition Algorithm 2, first subregion I is produced, then subregion II, and finally subregion III. Subregion III includes: H: 1→21, V: 17→24, and the corresponding GMoN is 0.4897. There is an overlap between subregion III and subregion II. So subregion III is adjusted manually to make each subregion distinct rectangle. The area covered by the dotted line in subregion II. MIMO nonlinear systems are much more complex than SISO nonlinear systems, and manual operations might be needed to aid the decomposition.

For comparison, the GMoNs of the local regions in [12] are $GMoN_1$=0.3688, $GMoN_2$=0.4215, $GMoN_3$=0.4624, and in [1] they are $GMoN_1$=0.4800, $GMoN_2$=0.4985, $GMoN_3$=0.3200.

Thus it can be seen that the decomposition in Table 3 is the most balanced. Moreover, the proposed decomposition is the simplest to implement since no repetitive tests of the threshold value or CLCS / OLMV tests are involved as a result of the use of GMoN.

3.5 A five-state MIMO non-isothermal biochemical reactor (fCSTR)

Consider a five-state MIMO control of a non-isothermal biochemical reactor [41-42]. Its mathematical model is given in (14).

$$\begin{cases} V_r\frac{dx_1}{dt} = Q_{01}C_{A0} - (Q_{01}+u_1)x_1 - \frac{V_r k_0 e^{-\frac{E}{Rx_4}} x_2^2 x_1}{k_m + x_1} \\ V_r\frac{dx_2}{dt} = Q_{02}C_{E0} - (Q_{01}+u_1)x_2 \\ V_r\frac{dx_3}{dt} = -(Q_{01}+u_1)x_3 + \frac{V_r Y_P k_0 e^{-\frac{E}{Rx_4}} x_2^2 x_1}{\bar{A}\, k_m + x_1} \\ \rho V_r C_P\frac{dx_4}{dt} = \rho C_P[Q_{01}T_{01} - (Q_{01}+u_1)x_4] - hA(x_4 - x_5) + \frac{\Delta H V_r k_0 e^{-\frac{E}{Rx_4}} x_2^2 x_1}{k_m + x_1} \\ \rho C_P V_c\frac{dx_5}{dt} = \rho C_P u_2(T_{02} - x_5) + hA(x_4 - x_5) \\ y = [\, x_3 \quad x_4] \end{cases} \tag{14}$$

The constants in Eq.(14) are given in [41-42]. The states are x_1, x_2, x_3, x_4, x_5; the inputs are u_1, u_2, and the outputs are x_3, x_4 ($y_1 = x_3$, $y_2 = x_4$). The inputs capture the system's nonlinearity at equilibrium and they are chosen as scheduling variables.

Applying the dichotomy method [12] to the fCSTR process, the gridding results are shown in Figure 8 and Figure 9. The GPs in u_1 direction are 54 GPs, and in u_2 direction there are 6 GPs.

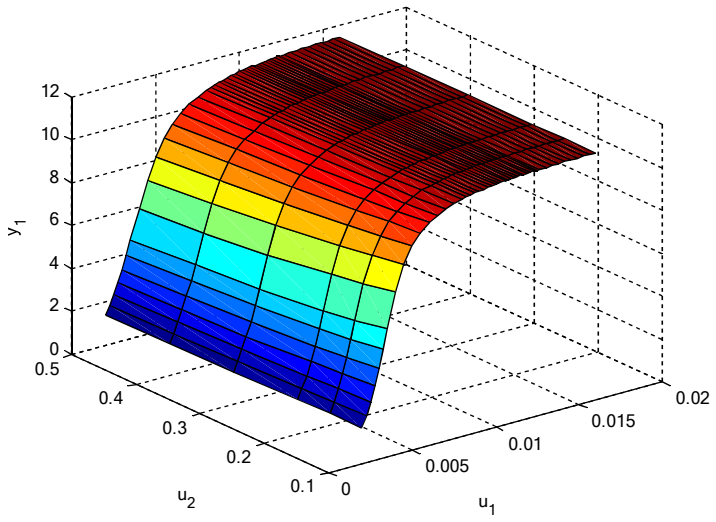

Figure 8. Gridding of fCSTR (y_1)

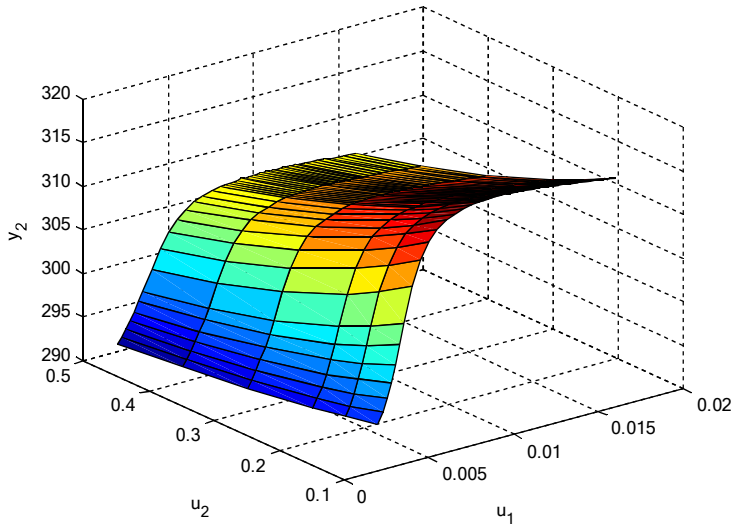

Figure 9. Gridding of fCSTR (y_2)

Based on the gridding result, the GMoN of the fCSTR system is computed according to (7) and (8).

$$\mathrm{GMoN} = 0.9785$$

Since it is larger than 0.6, we apply the proposed Algorithm 2 to this fCSTR with $\xi_0 = 0.6$ and step-length $\zeta = 0.01$. The decomposition is shown in Figure 10. Details of the decomposition are summarized in Table 4.

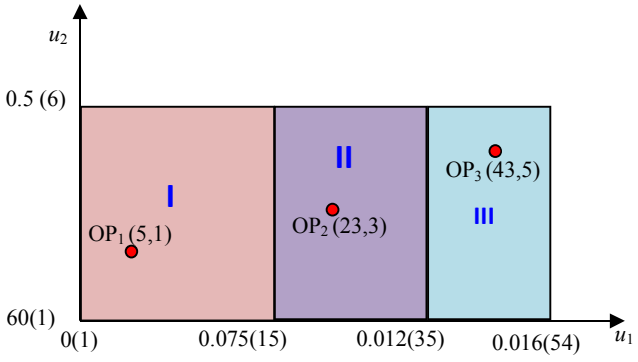

Figure 10. Self-balanced decomposition result of the fCSTR process

Table 4 Self-balanced multi-model decomposition of the fCSTR with final threshold $\xi = 0.55$

Subregion	1st	2nd	3rd
Linearized models	H:1→15 V:1→6	H:16→35 V: 1→6	H:36→47 V: 1→6
Operating point of BLLM (x,u)	OP_1 (5,1) ([9.6, 0.21, 4.2, 301.73, 301.65]', [0.003; 0.1])	OP_2 (23,5) ([0.76,0.69,11.2,313.9, 313.6]', [0.0098;0.2])	OP_3 (43,5) ([0.42,1.0,11.4,307.6 307.2]', [0.015;0.4])

Subrange	$\begin{cases}0.002 \le u_1 < 0.0075 \\ 0.1 \le u_2 < 0.5\end{cases}$	$\begin{cases}0.0075 \le u_1 < 0.012 \\ 0.1 \le u_2 < 0.5\end{cases}$	$\begin{cases}0.012 \le u_1 < 0.016 \\ 0.1 \le u_2 < 0.5\end{cases}$
GMoN	0.5458	0.5369	0.5278

As can be seen in Table 4, the decomposition of the fCSTR system is balanced with respect to GMoN. If the MMD methods in [12] [1] are used to decompose the fCSTR process, we also get three subregions. And the GMoNs are: $GMoN_1$=0.4277, $GMoN_2$=0.4365, $GMoN_3$=0.5212, and $GMoN_1$=0.5436 $GMoN_2$=0.5471, $GMoN_3$=0.4213.

3.6 Discussion

To eliminate the drawbacks in the current methods and obtain a balanced model bank, a self-balanced multi-model decomposition method is proposed for both SISO and MIMO nonlinear systems. Two SISO systems and two MIMO systems have been investigated using the proposed SBMMD and compared to some former gap-based decomposition methods. It is illustrated that the proposed method can be implemented comparatively more easily with less tuning and the decomposition result is more balanced in terms of GMoN. Besides, reliance on prior knowledge has been decreased as a result of the iterative mechanism, and the balanced decomposition results are evident during the decomposition process as the GMoN is used as a division criterion. What is more, the division process is implemented almost automatically.

In the next sections, BMMPCs will be designed based on the balanced decomposition results, and closed-loop control simulations will show how the balanced decomposition improves the closed-loop performance.

4. BMMPC for nonlinear systems

In this work, the MMPC is designed based on the balanced decomposition and it is thus denoted as the balanced MMPC (BMMPC) method to differentiate from other MMPC methods.

4.1 Local MPC design

After self-balanced multi-model decomposition, a linear model bank is set up with m local linear models P_j (j = 1, 2, …, m) to approximate nonlinear system (2). The state-space model of P_j is represented by (15).

$$\begin{cases} x_j'(k+1) = A_j x_j'(k) + B_j u_j'(k) \\ y_j'(k) = C_j x_j'(k) + D_j u_j'(k) \end{cases}, \quad j = 1, 2, \ldots, m \tag{15}$$

where $x_j'(k)$ is the state; $x_j'(k) = x(k) - x_{0j}$, $u_j'(k) = u(k) - u_{0j}$, $y_j'(k) = y(k) - y_{0j}$; A_j, B_j, C_j, and D_j are the linearized and discretized state-space model matrices of P_j around the jth steady state point (x_{0j},u_{0j}, y_{0j}) of system (2) .

A local MPC is designed based on (15) using the following objective function [1]:

$$J_j = \sum_{i=1}^{N_{yj}} \left\| r_j'(k+i) - y_j'(k+i) \right\|_{Q_j}^2 + \sum_{i=0}^{N_{uj}-1} \left\| \Delta u'_j(k+i) \right\|_{R_j}^2 \tag{16}$$

subject to

$$\begin{cases} u'_{j,min} \le u'_j \le u'_{j,max} \\ \Delta u'_{j,\min} \le \Delta u'_i \le \Delta u'_{j,\max} \\ y'_{j\min} \le y'_j \le y'_{j\max} \end{cases} \tag{17}$$

where Q_j and R_j denote weighting matrices; N_{yj} and N_{uj} denote prediction and control horizons; and r_j' denotes the reference, j = 1, 2… m. These parameters will be tuned to satisfy the local stability and control performance requirements.

Solving the Quadratic Programming (QP) problem [43] formed by (14)-(16) using the QP solver in MATLAB, the solution at time instant k is obtained, which guarantees the closed-loop stability of local linear system P_i [43]:

$$u'_j(k) = u'_j(k-1) + \Delta u'_j(k) \tag{18}$$

Thus, the control input of MPC$_j$ is acquired as in (18).

$$u_j(k) = u'_j(k) + u_{j0} \tag{19}$$

4.2 Controller combination of BMMPC

To combine the local MPCs (designed using the balanced models) into a MMPC, namely a BMMPC, the weighting method from [44] is employed here.

At time instant k, the scheduling variable is marked as θ_k; the equilibrium point corresponding to θ_k is (x_{0k}, u_{0k}, y_{0k}); and the linearized model of the nonlinear system (2) about (x_{0k}, u_{0k}, y_{0k}) is noted as P_k. Then at time instant k, the weight for MPC$_j$ is computed by (20).

$$\varphi_j(\theta_k) = \frac{(1-\delta(P_j,P_k))^{k_g}}{\sum_i^m (1-\delta(P_i,P_k))^{k_g}}, \quad j = 1,\ldots, m. \tag{20}$$

where $\delta(P_j,P_k)$ is the gap between P_k and the jth local linear system P_j; $k_g \geq 1$ is a tuning parameter; and the summation of the m weights is equal to 1.

Then the BMMPC's output is computed by (21).

$$u(k) = \sum_j^m \varphi_j(\theta_k) u_j(k) \tag{21}$$

The structure of the proposed BMMPC for nonlinear systems is shown in Figure 11. The BMMPC will be implemented to the three CSTRs to illustrate the effectiveness of the proposed methods in Section 5.

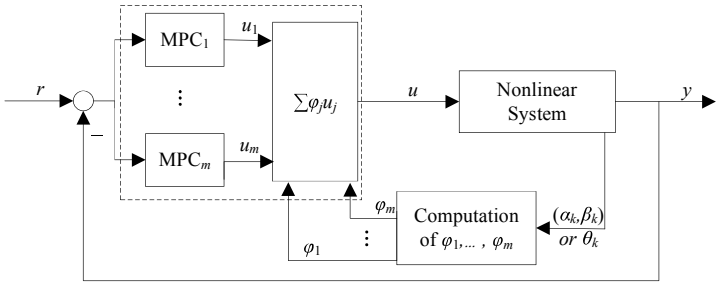

Figure 11. BMMPC for nonlinear systems based on the GMoN

5 Simulations

Case 1: The eCSTR process

For the eCSTR process, based on the balanced decomposition result obtained by Algorithm 1, three local linear MPCs are tuned separately to satisfy the stability and control performance. Namely, Q_j, R_j, N_{yj}, N_{uj} are selected separately. Then after combination according to Eqs.(19) and (20), a BMMPC, denoted as BMMPC$_1$, is obtained for closed-loop simulation in Figure 12. Where y_1 is the eCSTR system's output under the proposed BMMPC$_1$, with the control input u_1. For comparison, two other MMPCs are designed with the same tuning parameters as BMMPC$_1$. MMPC$_2$ is designed based on the decomposition from [17], which is a less balanced division. Its output and input are denoted as y_2 and u_2, respectively, in Figure 12. MMPC$_3$ uses the

decomposition result from [15], which is also a less balanced division, with its output and input denoted as y_3 and u_3 in Figure 12.

The closed-loop performance of the three MMPCs can be clearly seen in Figure 12. As a whole, the three MMPCs all perform well, especially for the middle stages. However, at the first stage, $MMPC_3$ is not as accurate as others. At the last stage, both $MMPC_2$ and $MMPC_3$ react to the change of reference signal slowly while the proposed $BMMPC_1$ is faster and more accurately. In order to differentiate the three MMPCs more precisely, their Integrated Absolute Error (IAE) values are calculated: IAE_1 = 31.2131(for $BMMPC_1$) and IAE_2 = 38.9297(for $MMPC_2$), IAE_3 = 39.7322(for $MMPC_3$). The values of the MPC objective functions are: J_1 = 22555; J_2 = 23517; J_3 = 24231. Hence, $BMMPC_1$ based on a balanced decomposition is better than $MMPC_2$ and $MMPC_3$ based on unbalanced model banks. The balanced model bank helps improve the closed-loop performance of an MMPC.

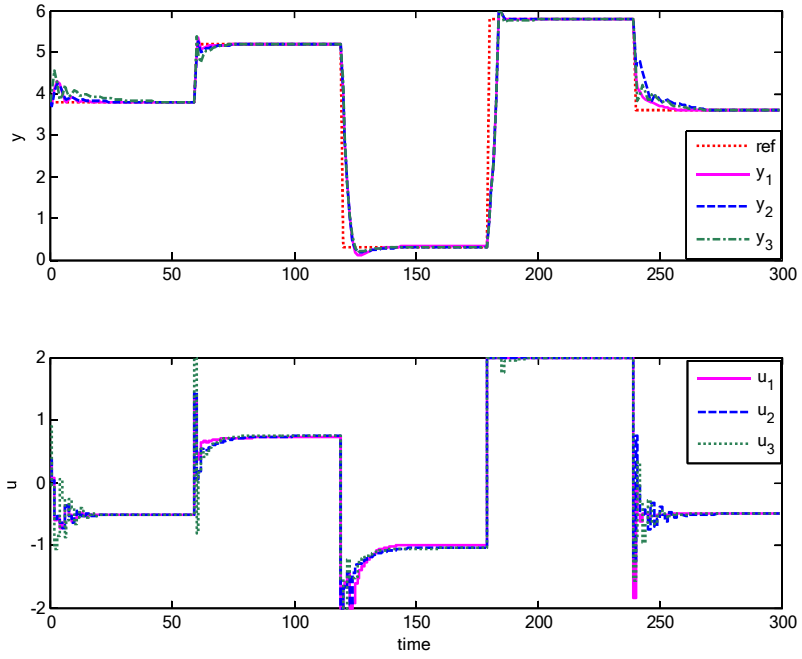

Figure 12. Closed-loop performance of eCSTR under 3 MMPCs

Case 2. The iCSTR process

For the iCSTR system, a BMMPC ($BMMPC_1$) is designed based on the balanced decomposition result with its input u_1 and output Ca_1, where the local parameters Q_j, R_j, N_{yj}, N_{uj} are chosen with different values to maximize the control performance. Another MMPC ($MMPC_2$) is designed using the decomposition in [15] to make a comparison. The input and output of iCSTR under are denoted as u_2 and Ca_2. A third MMPC ($MMPC_3$) is designed using the decomposition in [17] with u_3 and Ca_3. $MMPC_2$ and $MMPC_3$ are designed with the same tuning parameters as $BMMPC_1$

The set-point tracking control responses are shown in Figure 13. As a whole, the three MMPCs perform well in the entire operating region: the outputs track the reference fast and accurately. With detailed observation, it is seen that Ca_3 has bigger overshoots when the set-point

changes; and during the lower and higher operating levels at the last two stages, $BMMPC_1$ is faster than $MMPC_2$ and $MMPC_3$. So the unbalanced MMPCs perform well during the middle operating level, but degrade when the set-point goes away from the middle operating level. The IAE values of the MMPCs for iCSTR are given to show the difference among the MMPCs. IAE_1 = 0.6771 (for $BMMPC_1$), IAE_2 = 2.0876 (for $MMPC_2$) and IAE_3 = 1.9023 (for $MMPC_3$). The values of the objective functions are: J_1 = 93.76; J_2 = 100.91; J_3 = 156.56. Thus these values confirm that the proposed BMMPC is better than common MMPCs.

For this example, it can be concluded that the balanced decomposition makes the local controllers have similar performance and further makes the BMMPC have consistently good performance. However, for $MMPC_2$ and $MMPC_3$, as the local controllers have quite different performance, after combination, the unbalanced MMPCs perform well in some operating region while badly in other operating region. Hence the balanced division of the nonlinear system is helpful for MMPC of a nonlinear system.

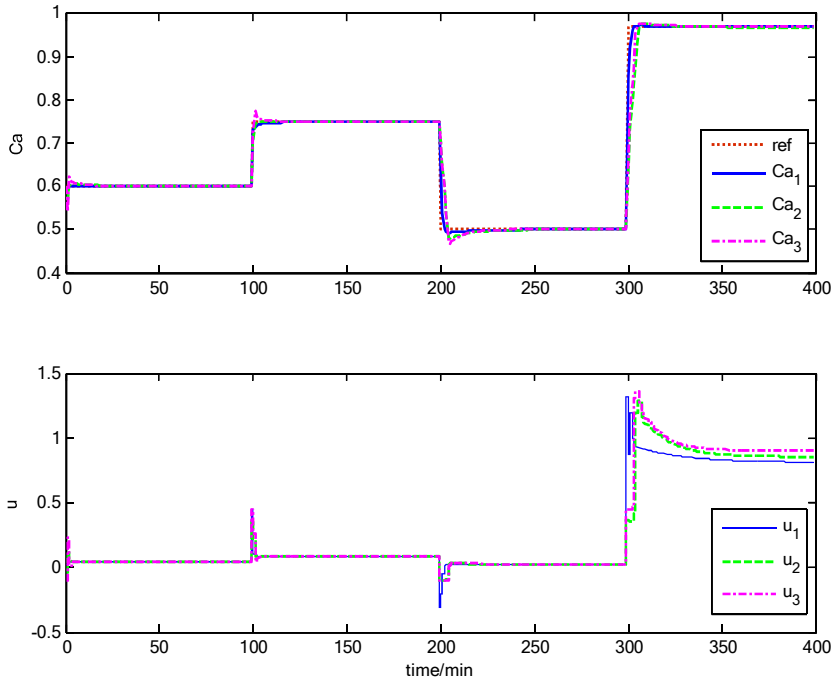

Figure 13. Closed-loop responses of iCSTR under 3 MMPCs

Case 3. The mCSTR process

In comparison with [12] and [1], the mCSTR system is also decomposed into three subregions, but more balanced, since the three subregions have similar GMoN values. Based on the balanced model bank in Table 3, three linear MPCs are designed and combined into a $BMMPC_1$ for set-point tracking control (see Figures 14-15). For the three linear MPCs, the control parameters Q_j, R_j, N_{yj}, N_{uj} are tuned separately to satisfy the control requirements. The outputs of the mCSTR under $BMMPC_1$ are denoted as C_{A1} and T_1, and the inputs are q_1 and q_{c1}. For comparison, two other MMPCs are designed with the same parameters as $BMMPC_1$. $MMPC_2$ is designed based on the division result from [12], for set-point tracking control with outputs C_{A2}, T_2 and inputs q_2, q_{c2}. $MMPC_3$ is designed based on the division result from [1] with

outputs C_{A3}, T_3 and inputs q_3, q_{c3}.

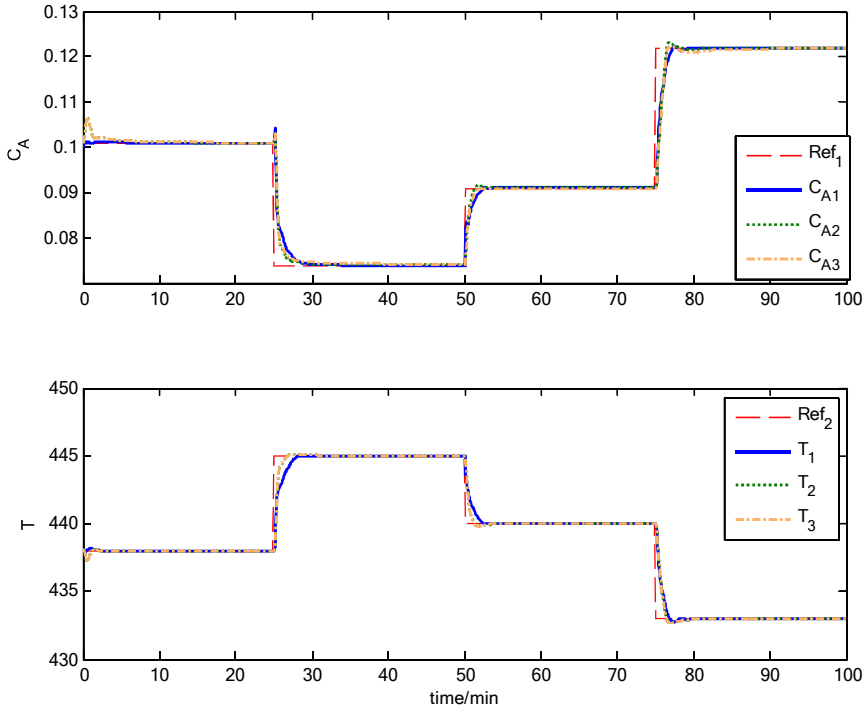

Figure 14. Closed-loop outputs of mCSTR under three MMPCs

Overall, the three MMPCs perform well: tracking the outputs quickly and precisely. After close observation, it is seen that C_{A1} and T_1 are more accurate than those of the other two MMPCs, although $MMPC_2$ and $MMPC_3$ are slightly faster than $BMMPC_1$ around *time* = 25min and *time* = 50min. On the other hand, $BMMPC_1$ performs much better than the other two at the beginning of the simulation. Using the normalized IAE [12], the IAEs of the three MMPCs can be computed: IAE_1=7.3901, IAE_2=9.3589, IAE_3= 9.3034. The values of the objective functions are: J_1 = [19325; 311862]; J_2 = [19531; 354825]; J_3 = [19524; 382325]. Therefore, the proposed BMMPC has consistent performance as the balanced decomposition helps improve the closed-loop performances.

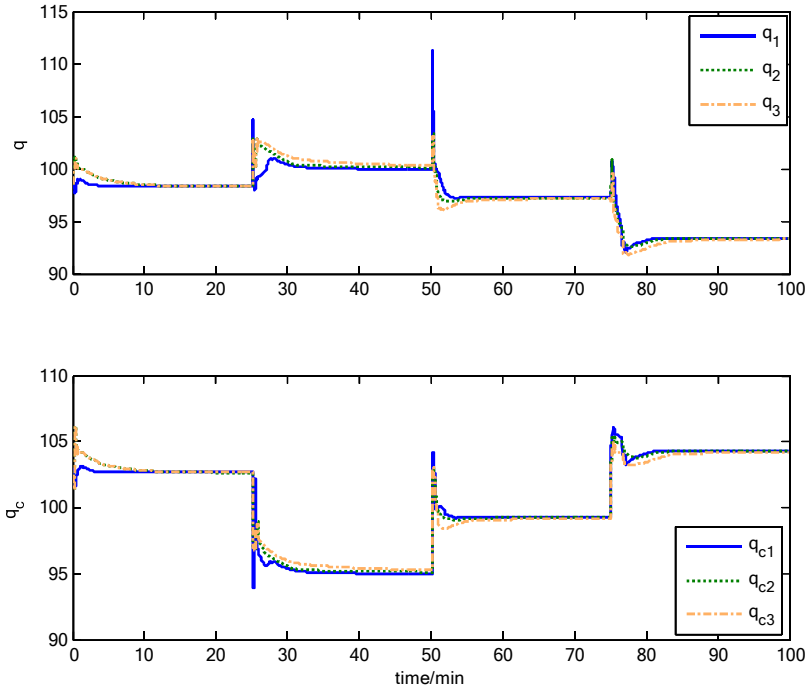

Figure 15. Closed-loop inputs of mCSTR under three MMPCs

Case 4. The fCSTR process

Based on the balanced model bank in Table 4, three linear MPCs are designed and combined into a $BMMPC_1$ for set-point tracking control (Figures 16-17). The control parameters of the three linear MPCs, Q_j, R_j, N_{yj}, N_{uj} are tuned separately to satisfy the control requirements. The outputs of the fCSTR under $BMMPC_1$ are denoted as y_{11} and y_{12}, and the inputs are u_{11} and u_{12}. For comparison, a nonlinear MPC (NPMC)[45] is designed for set-point tracking control with outputs y_{21}, y_{22} and inputs u_{21}, u_{22}, where the SQP method is used to solve the NMPC problem.

As seen in Figures 16-17, the two pairs of outputs track the set-point signals closely, and the two controllers perform both well. However, the BMMPC is slightly faster than the NMPC. Besides, y_{21} and y_{22} have bigger overshoots than y_{11} and y_{12}. Using the normalized IAE [12], the IAEs are computed: IAE_1=11.5073, IAE_2=23.8775. The values of the objective functions are: J_1 = [365812; 58235]; J_2 = [373882; 620696]. For the fCSTR system, the reason that the proposed BMMPC outperforms the NMPC is partly because the BMMPC is designed based on the balanced decomposition and its local MPCs are tuned separately, and partly because the QP solver in the MMPC finds the optimal solutions while the SQP may find the suboptimal solutions.

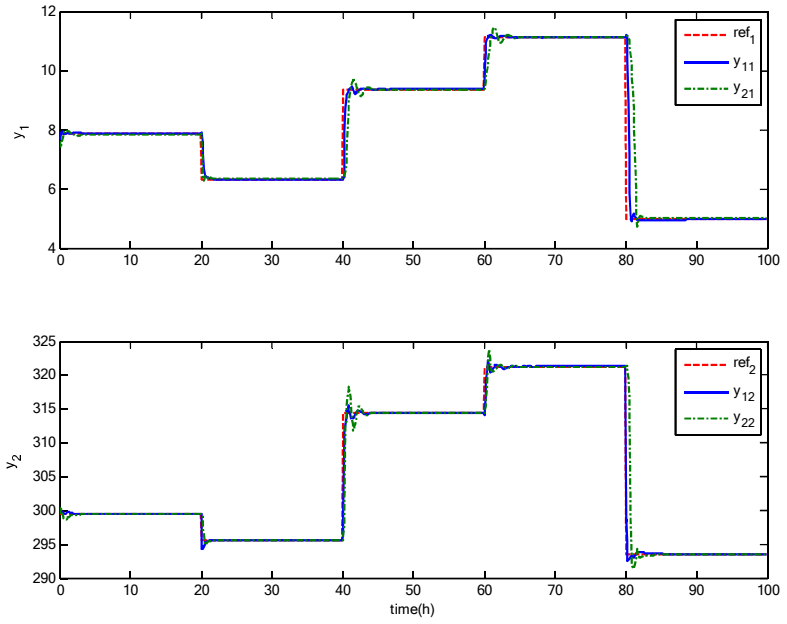

Figure 16. Closed-loop outputs of fCSTR under the BMMPC and NMPC

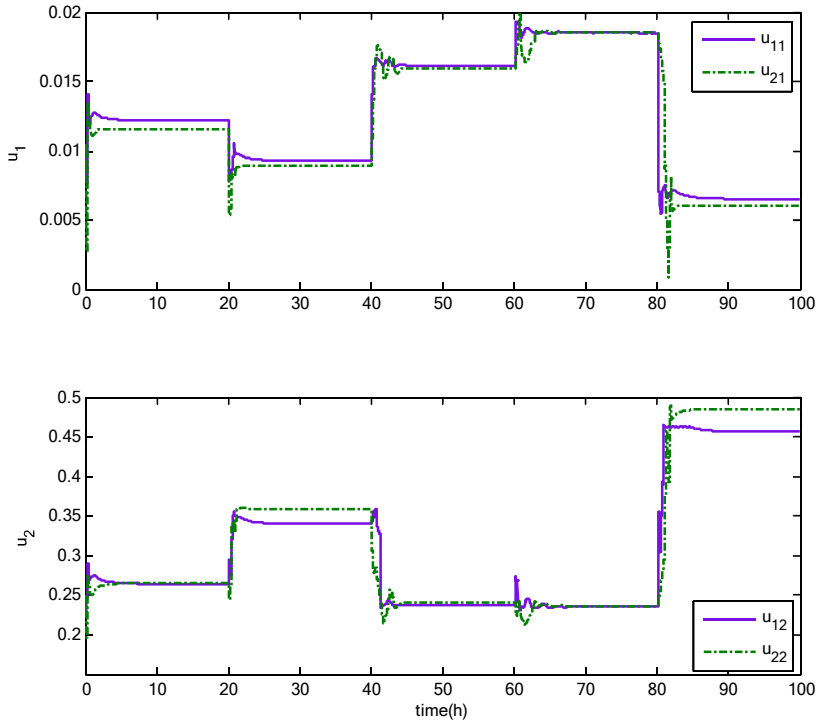

Figure 17. Closed-loop inputs of fCSTR under the BMMPC and NMPC

6 Conclusions

MMD is an important element for MMPC of nonlinear systems and the MMD result has a

direct influence on the closed-loop performance. An SBMMD method is proposed based on the GMoN for both SISO and MIMO nonlinear systems. Thus a nonlinear system can be partitioned into multiple balanced linear sub-models easily without complicated, repetitive parameter tuning. The subregions all have smaller GMoNs than the whole region. The decomposition reduces the nonlinearity of the subregions, and thus simplifies the local controller design. Besides, the balanced decomposition helps make the local controller have more similar performance and further improves the closed-loop performance of BMMPC. Four CSTR processes are investigated to illustrate the use of the SBMMD and the implementation of the BMMPC. Closed-loop simulations demonstrate that the resulted BMMPC has better and more consistent performance than common MMPCs. However, when the considered system has three or more scheduling variables, the application of the proposed SBMMD will involve much more complicated computation. Therefore, improvement of the SBMMD for systems with more than two scheduling variables is still under study. Besides, the closed-loop stability of the multi-model approach should be further study to get the appropriate number of local models that can guarantee the nonlinear system's stability.

Acknowledgments

This work is supported by the Fundamental Research Funds for Central Universities (B200202214), and by the Research Fund from Science and Technology on Underwater Vehicle Technology Laboratory (No.6142215200102), National Key R&D Program (2017YFC0306100). Primary Research & Development Plan of Jiangsu Province (E2019649), Science and Technology Support Plan-Project Foundation of Changzhou (CE20215017).

References

[1] Du J, Johansen TA. Integrated Multilinear Model Predictive Control of Nonlinear Systems Based on Gap Metric. Industrial & Engineering Chemical Research 2015, 54 (22): 6002–6011.

[2] Hernandez A, Ruiz F, Gusev S, Keyser R, Quoilin S, Lemort V. Experimental validation of a multiple model predictive control for waste heat recovery organic Rankine cycle systems. Applied Thermal Engineering 2021, 193: 1-12.

[3] Du X, Yu P, Ren C. Clustering Multi-model generalized predictive control and its application in wastewater biological treatment Plant. Journal of Applied Sciences 2013, 13(21): 4869-4874.

[4] Cao R, Wan H, He Z, Lu Y. Multiple model predictive control of perching maneuver based on guardian maps. Chinese Journal of Aeronautics 2021, in press.

[5] Tao X, Li D, Wang Y, Li N, Li S. Gap-metric-based multiple-model Predictive control with a polyhedral stability region. Industrial & Engineering Chemical Research 2015, 54: 11319-11329.

[6] Chi Q, Liang J. A multiple model predictive control strategy in the PLS framework. Journal of Process Control 2015, 25: 129-141.

[7] Du J, Zhang L. Included-Angle-Based Decomposition and Weighting in Multi-model Predictive Control of Hammerstein Systems. Industrial & Engineering Chemical Research 2017, 56: 11270–11280.

[8] Du J, Zhang L, Chen J, Li J, Zhu C. Multi-model predictive control of Hammerstein-Wiener systems based on balanced multi-model partition. MATHEMATICAL AND COMPUTER

MODELLING OF DYNAMICAL SYSTEMS 2019, 25(4): 333-353.

[9] Du J, Zhang L, Chen J, Jiang X, Zhu C. Self-adjusted decomposition for multi-model predictive control of Hammerstein systems based on included angle. ISA Transactions 2020, 103**:** 19–27.

[10] Murray-Smith R, Johansen T A. Multiple model approaches to modeling and control. Taylor & Francis: London, England, 1997.

[11] Galán O, Romagnoli JA, Palazoglu A, Arkun Y. Gap metric concept and implication for multilinear model-based controller design. Industrial & Engineering Chemical Research 2003, 42: 2189-2197.

[12] Du J, Song C, Yao Y, Li P. Multilinear model decomposition of MIMO nonlinear systems and its implication for multilinear model-based control. Journal of Process Control 2013, 23: 271-281.

[13] Tan W, Marquez HJ, Chen T, Liu J. Multimodel analysis and controller design for nonlinear processes. Computers and Chemical Engineering 2004, 28: 2667-2675.

[14] Hosseini SM, Fatehi A, Johansen TA, Sedigh AK. Multiple model bank selection based on nonlinearity measure and H-gap metric. Journal of Process Control 2012, 22:1732-1742.

[15] Du J, Song C, Li P. Application of gap metric to model bank determination in multilinear model approach. Journal of Process Control 2009, 19: 231-240.

[16] Du J, Johansen TA. Integrated Multimodel Control of Nonlinear Systems Based on Gap Metric and Stability Margin. Industrial and Engineering Chemical Research 2014, 53(24): 10206–10215.

[17] Du J, Johansen TA. Control-relevant nonlinearity measure and integrated multi-model control. Journal of Process Control 2017, 57:127-139.

[18] Song C, Wu B, Zhao J, Li P. An integrated state space partition and optimal control method of multi-model for nonlinear systems based on hybrid systems. Journal of Process Control 2015, 25: 59-69.

[19] Daoutidis P, Tang WT, Jogwar S. Decomposing complex plants for distributed control-perspectives from network theory. Computers and Chemical Engineering 2018 (114): 43-51.

[20] Tang W, Allman A, Pourkargar DB, Daoutidis P. Optimal decomposition for distributed optimiztion in nonlinear model predictive control through community detection. Computers and Chemical Engineering 2018 (116): 144-155.

[21] Mitrai I, Daoutidis P. Decomposition of integrated scheduling and dynamic optimization problems using community detection. Journal of Process Control 2020 (90): 63-74.

[22] Shin S, Zavala VM, Anitescu M. Decentralized schemes with overlap for solving Graph-Structured optimization problems. IEEE Transactions on Control of Networks Systems. 2020 (7): 1225-1236.

[23] Shin S, Anitescu M, Zavala VM. Overlapping Schwarz decomposition for constrained quadratic programs. 59th IEEE Conference on Decision and Control, Jeju Island, Korea, 2020, 3004-3009.

[24] Georgiou TT, Smith MC. Optimal robustness in the gap metric. IEEE Transactions on Automatic Control 1990, 35 (6): 673-686.

[25] El-Sakkary AK. The gap metric: Robustness of stabilization of feedback systems. IEEE Transaction on Automatic Control 1985, 30 (3): 240-247.

[26]Guay M, McLellan PJ, Bacon DW. Measurement of nonlinearity in Chemical Process Control Systems: The Steady State Map. The Canadan Journal of Chemical Engineering 1995, 73: 868-882.

[27]Schweickhardt T, Allgower F. Linear control of nonlinear systems based on nonlinearity measures. Journal of Process Control 2007, 17: 273-28.

[28]Nikolaou M, Misra P. Linear control of nonlinear process: recent developments and future directions. Computers and Chemical Engineering 2003, 27:1043-1059.

[29]Helbig A, Marquardt W, Allgower F. Nonlinearity measures: definition, computation and applications. Journal of Process Control 2000, 10: 113-123.

[30]Schweickhardt T, Allgower F. On system gains, nonlinearity measures, and linear models for nonlinear systems. IEEE Transactions on Automatic Control 2009, 54(1): 62-78.

[31]Harris KR, Colantonio MC, Palazoglu A. On the computation of a nonlinearity measure using functional expansions. Chemical Engineering Science 2005, 55: 2393-2400.

[32]Sun D, Hoo KA. Nonlinearity measure for a class of SISO nonlinear systems. International Journal of Control 2000, 73: 29-37.

[33]Desoer CA, Wang YT. Foundations of feedback theory for nonlinear dynamical systems. IEEE Transaction Circuits and Systems 1980, 27: 104-123.

[34]Liu Y, Li XR. Measure of nonlinearity for estimation. IEEE Transactions on Signal Processing 2015, 63(9): 2377-2388.

[35]Guay, M. The effect of process nonlinearity on linear controller performance in discrete-time systems. Computers and Chemical Engineering 2006, 30: 381-391.

[36]Liu J, Meng Q, Fang F. Minimum variance lower bound ration based nonlinearity measure for closed loop systems. Journal of Process Control 2013, 23: 1097-1107.

[37]Tan GT, Huzmezan M, Kwok KE. Vinicombe metric as a closed-loop nonlinearity measure. European Control Conference, Cambridge, UK, 2003, 751-756.

[38]Du J, Song C, Li P. A Gap metric based nonlinearity measure for chemical processes. Proceedings of the 2009 American Control Conference, St. Louis, MO, US, 2009**,** 4440-4445.

[39]Du J, Tong Z. An improved nonlinearity measure based on gap metric. Proceedings of the 33rd Chinese Control Conference, Nanjing, China, 2014, 1920-1923.

[40]Rugh WJ, Shamma JS. Research on gain scheduling, Automatica 2000, 36: 1401-1425.

[41]Garcia-Alvarado MA, Ruiz-Lopez II, Torres-Ramos T. Tuning of multivariate PID controllers based on characteristic matrix eigenvalues, Lyapunov functions and robustness criteria. Chemical Engineering Science 2005 (60): 897-905.

[42]Carrillo-Ahumada J, Rodriguez-Jimenes GC, Garcia-Alvarado MA. Tuning optimal-robust linear MIMO controllers of chemical reactors by using Pareto optimality. Chemical Engineering Journal 2011(174): 357-367.

[43] Maciejowski JM. Predictive control: with constraints. Harlow, UK: Pearson Education Limited; 2002.

[44]Du J, Johansen TA. A gap metric based weighting method for multimodel predictive control of MIMO nonlinear systems. Journal of Process Control 2014, 24: 1346-1357.

[45] Grune J, Pannek J. Nonlinear model predictive control: Theory and Algorithm. Switzerland, Springer International Publishing, 2017.

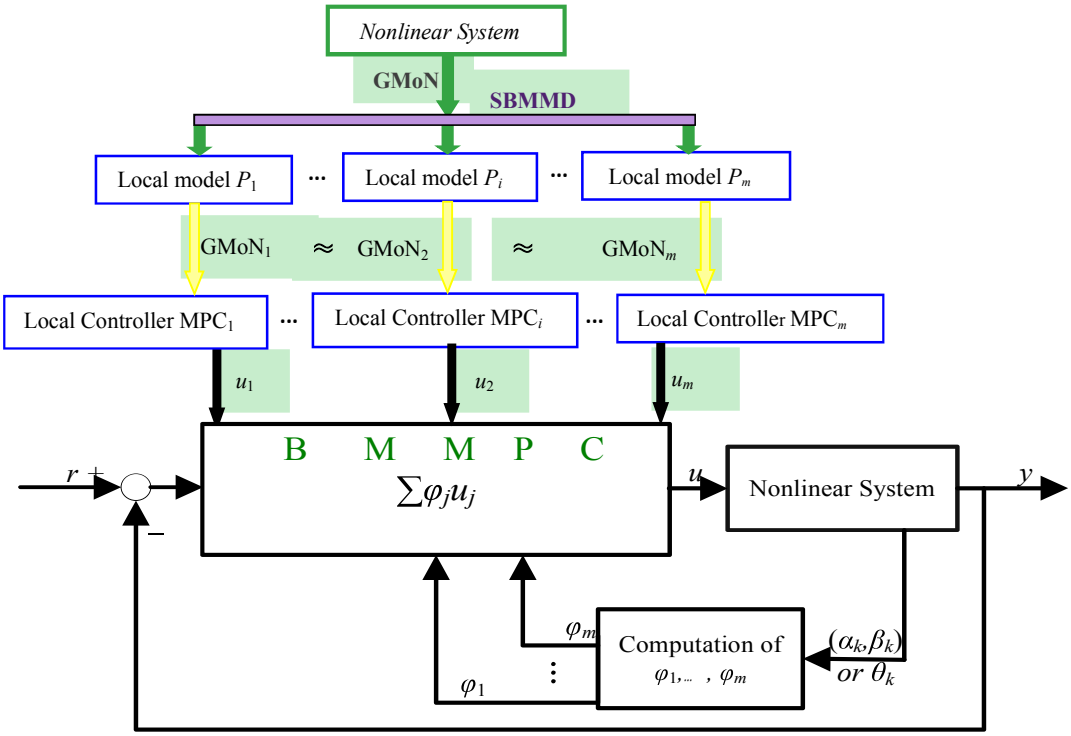
Nonlinear System
GMoN
SBMMD
Local model P_1
Local model P_i
Local model P_m
$GMoN_1$ ≈ $GMoN_2$ ≈ $GMoN_m$
Local Controller MPC_1
Local Controller MPC_i
Local Controller MPC_m
u_1
u_2
u_m
B M M P C
$\sum \varphi_j u_j$
r
+
−
u
Nonlinear System
y
φ_m
φ_1
Computation of
$\varphi_1, \ldots, \varphi_m$
(α_k, β_k)
or θ_k